ARTICLES
PUBLISHED ONLINE: 11 MAY 2014 | DOI: 10.1038/NNANO.2014.84
nature nanotechnology

In vivo endothelial siRNA delivery using polymeric nanoparticles with low molecular weight

James E. Dahlman and Carmen Barnes *et al.**

Dysfunctional endothelium contributes to more diseases than any other tissue in the body. Small interfering RNAs (siRNAs) can help in the study and treatment of endothelial cells *in vivo* by durably silencing multiple genes simultaneously, but efficient siRNA delivery has so far remained challenging. Here, we show that polymeric nanoparticles made of low-molecular-weight polyamines and lipids can deliver siRNA to endothelial cells with high efficiency, thereby facilitating the simultaneous silencing of multiple endothelial genes *in vivo*. Unlike lipid or lipid-like nanoparticles, this formulation does not significantly reduce gene expression in hepatocytes or immune cells even at the dosage necessary for endothelial gene silencing. These nanoparticles mediate the most durable non-liver silencing reported so far and facilitate the delivery of siRNAs that modify endothelial function in mouse models of vascular permeability, emphysema, primary tumour growth and metastasis.

The vascular system releases factors into the bloodstream, changes the expression of specific receptors, modifies intercellular junctions, and regulates the immune response[1]. Endothelial cells also mediate biological functions such as endocytosis and metabolism[2]. Because these processes relate fundamentally to physiology, dysfunctional endothelium promotes more disease than any other tissue in the body[3]. Yet, modulating the behaviour of endothelial cells *in vivo* remains challenging, particularly in cases that require the inhibition of multiple endothelial genes.

RNAi-mediated modification of gene expression has the potential to improve disease treatment and *in vivo* studies of complex biological processes. However, its utility is limited by inefficient systemic delivery, with the exception of ionizable lipids and lipid-like compounds termed lipidoids, which reduce hepatic gene expression by 50% after injection of 0.01 mg kg^{-1} siRNA (refs 4–7). In contrast, efficient endothelial gene silencing without the transfection of hepatocytes has remained challenging. Although cationic lipids have been reported to deliver siRNA to endothelial cells, these endothelial delivery systems require cumulative doses of up to 7.5 mg kg^{-1} to achieve robust gene silencing[8–13].

Nanoformulations based on polymeric materials have delivered siRNA to hepatocytes and melanoma[14,15]. Unlike lipid-based nanoparticles, polymer–nucleic acid nanoparticles condense via multivalent interactions, leading to significantly different physical stabilities. One polymer class that has been investigated as a gene delivery material is polyethyleneimine (PEI)[16]. Although nanoparticles made from high-molecular-weight PEI ($M_w \approx 25{,}000$ Da) have delivered nucleic acids, they are associated with off-target effects[17]. In contrast, nanoformulations from low-molecular-weight PEI ($M_w \approx 600$ Da) are relatively well tolerated but cannot facilitate siRNA delivery[17,18].

Here, we report an siRNA–nanoparticle formulation that reduces endothelial gene expression by over 90% at a dose of 0.10 mg kg^{-1} and by 50% at doses as low as 0.02 mg kg^{-1}. This formulation, termed 7C1, differs from traditional lipid-based nanoparticle formulations because it can deliver siRNA to lung endothelial cells at low doses without substantially reducing gene expression in pulmonary immune cells, hepatocytes or peritoneal immune cells. We demonstrate that 7C1-mediated endothelial gene silencing affects function *in vivo* by using our nanoformulation to modify mouse models of vascular permeability, emphysema, lung tumour growth and lung metastasis.

Efficient siRNA delivery to endothelium *in vitro* and *in vivo*

A diverse library of epoxide-modified lipid–polymer hybrids were synthesized (Fig. 1a, Supplementary Fig. 1a). The compounds were tested for their ability to reduce gene expression in HeLa cells at four different lipid:siRNA mass ratios (2.5:1, 5:1, 10:1 and 15:1) (Supplementary Fig. 1b). HeLa cells expressing Firefly and Renilla luciferase were chosen as a first-pass screen for these 2,000 nanoparticles formulated with siLuciferase because of the cost-effectiveness of the assay[5]. We defined a successful nanoparticle as one that silenced Firefly luminescence by more than 70%, but decreased Renilla luminescence by less than 25%. Although only 0.9% of compounds in the library were successful at a mass ratio of 2.5, 6.5% were successful when the mass ratio was 15 (Table 1). We then measured Firefly luminescence as a function of lipids bound to successful PEI_{600} compounds. Luminescence decreased with the number of lipids bound (Supplementary Fig. 1c). A subset of formulations tested in HeLa cells were tested for their ability to deliver siRNA to human (HMVEC) and murine (bEnd.3) endothelial cells *in vitro*. The most effective compound, termed 7C1 based on its composition, reduced target mRNA expression by more than 85% in HeLa, HMVECs and bEnd.3 cells at a dose of 30 nM (Fig. 1b). Interestingly, 7C1 efficacy did not change with mass ratio in HeLa cells (Supplementary Fig. 1d). Only 2 nM was required to reduce target gene expression in bEnd.3 cells by 50%, and 7C1 did not affect bEnd.3 cell morphology or induce apoptosis *in vitro* at doses as high as 133 nM (Supplementary Fig. 1e,f).

7C1 was synthesized by reacting C_{15} epoxide-terminated lipids with PEI_{600} at a 14:1 molar ratio, and was formulated with $C_{14}PEG_{2000}$ to produce nanoparticles (diameter between 35 and 60 nm) that were stable in PBS solution for at least 40 days (Fig. 1c–e, Supplementary Fig. 1g–i). Particles formed multilamellar vesicles rather than the periodic aqueous compartments containing siRNA that make up stable nucleic-acid lipid particle formulations[19] (Fig. 1d, Supplementary Fig. 1j). Because particle charge at different values of pH can affect delivery by modifying interactions with

*A full list of authors and their affiliations appears at the end of the paper.

Table 1 | Per cent of compounds reducing Firefly luminescence more than 70% while not reducing Renilla luminescence more than 25% as a function of lipid:siFire mass ratio.

Compound:siFire mass ratio	Successful nanoparticles (%)
2.5	0.9
5	0.7
10	3.5
15	6.5

Table 2 | Intravenous dose required to reduce target gene mRNA expression by 50% *in vivo* (mg kg^{-1}) (ED_{50}).

Gene	Lung	Heart	Kidney
VEcad	0.02	0.04	0.08
ICAM2	0.02	0.08	0.15
Tie2	0.04	0.12	0.12
VEGFR-2*	0.05	0.10	0.25
Tie1*	0.05	0.10	0.15

*ED_{50} value calculated from multigene silencing experiment (Fig. 2d).

serum proteins, the zeta potential was measured for 7C1 formulated with siRNA at blood physiological pH (7.4) and pK_a (ref. 6; Fig. 1f). While 7C1 formed electrically neutral particles at pH 7.4, its pK_a was 5.0. This value is different than the pK_a of particles optimized for hepatocyte delivery[20].

We investigated the serum kinetics and biodistribution of 7C1 siRNA nanoparticles *in vivo*. 7C1 was complexed with Alexa647-tagged siRNA and injected intravenously. After 1 h, skin tissue whole-mounted for confocal microscopy showed colocalization between 7C1 and endothelial cells, suggesting endothelial cells endocytosed 7C1 *in vivo* (Fig. 1g). Endothelial cell uptake was confirmed by an increase in Alexa647 mean fluorescence intensity in endothelial cells sorted from pulmonary tissue 1 h after injection with 7C1 formulated with Alexa647-tagged siRNA (Fig. 2g). 7C1 serum kinetics was then measured. 7C1 serum concentration decreased by 50% within 20 min of intravenous injection, indicating the formulation was rapidly cleared or endocytosed (Fig. 1h). To investigate 7C1 biodistribution, Cy5.5 fluorescence was quantified 4 and 24 h after injection (when 7C1 serum concentrations were negligible) (Fig. 1i). Renal fluorescence was high, indicating that the kidneys aid in the clearance of siRNA delivered by 7C1. *In vitro*, HMVECs take up 7C1 via caveolae- and clathrin-mediated endocytosis (Fig. 2a).

To confirm that endothelial localization resulted in functional siRNA delivery, mRNA was measured after 7C1 was formulated with siRNAs targeting genes expressed primarily by endothelial cells. 7C1 was formulated with siRNA targeting the gene ICAM-2 and injected with a dose of 0.6 mg kg^{-1} on day one and four. Five days later, skin was analysed with confocal microscopy and flow cytometry (Supplementary Fig. 2a,b). ICAM-2 expression on lymph node and omentum endothelial cells was also measured with flow cytometry (Supplementary Fig. 2b). ICAM-2 expression decreased compared with PBS- and siLuciferase- (termed siCntrol) treated mice. 7C1 was then formulated with 0.60, 0.05, 0.02 or 0.007 mg kg^{-1} si-ICAM2 and injected once (Fig. 2b). Because ICAM-2 is principally expressed by endothelial cells in all major tissue beds, this assay detects endothelial gene silencing in any organ[21]. 7C1 reduced ICAM-2 mRNA expression in the pulmonary, cardiovascular and renal endothelium by 50% at doses of 0.02, 0.08 and 0.15 mg kg^{-1}, respectively (Fig. 2b, Table 2). To ensure efficient delivery was not limited to siICAM-2, we measured gene silencing in mice treated with siRNA targeting VE-cadherin (VEcad), a junctional protein whose expression is limited to endothelium. Cardiovascular, renal and pulmonary VEcad mRNA decreased by 50% at doses of 0.04, 0.08 and less than 0.02 mg kg^{-1}, respectively (Fig. 2c, Table 2). 7C1-siVEcad also reduced VEcad protein levels in whole-lung homogenates at 0.03 mg kg^{-1} (Fig. 2d). We then investigated whether reduced VEcad protein levels increased vascular permeability. Compared with mice treated with PBS or siCntrol, the extravasation of Evans Blue Dye out of the pulmonary vasculature increased 2.5-fold seven and fourteen days after a single 0.6 mg kg^{-1} injection of siVEcad (Fig. 2e). These data demonstrate that 7C1 facilitates the most efficient non-liver siRNA delivery reported to date.

Because *in vivo* multigene silencing requires highly efficient delivery, it has been limited to hepatocytes[5]. 7C1 silenced five endothelial genes (Tie1, Tie2, VEcad, VEGFR-2 and ICAM-2) concurrently. Three days following intravenous injection with a total dose of 0.25 mg kg^{-1}, target mRNA of all five genes decreased between 60% and 80% in pulmonary vasculature (Fig. 2f, Supplementary Fig. 2c–e). Target gene expression remained constant after siCntrol was injected (total dose of 2.0 mg kg^{-1}), suggesting that the reduced mRNA levels were due to RNAi. To our knowledge, this is the first demonstration of multi-gene silencing in endothelial cells *in vivo*.

Efficient delivery also facilitates durable gene silencing, because the duration of gene silencing is generally dose-dependent[5]. mRNA silencing was measured as a function of time after a 0.6 mg kg^{-1} injection of siICAM-2 (Fig. 2g). Pulmonary ICAM-2 mRNA expression initially decreased by 92% and remained suppressed by between 73% and 85% for 21 days. By contrast, cardiovascular and renal endothelial ICAM-2 expression increased continually over the first 28 days, reaching 50% of initial expression after day ten, again suggesting less efficient endothelial cell delivery in these vascular beds compared with lung endothelium (Fig. 2g). We then measured gene silencing in different organs after modifying the particle size and 7C1:siRNA mass ratio (see Supplementary Section '7C1 biophysical optimization'; Supplementary Fig. 2f–i)). 7C1 was complexed with siRNA targeting the endothelial specific gene Tie2 (ref. 21). In all cases, the most potent delivery was measured in pulmonary endothelial cells (Supplementary Fig. 2f–i).

Although others have reported siRNA delivery to the lung, functional gene silencing required doses much higher than 0.02 mg kg^{-1}. Because the relative silencing in different cell types dictates the type of *in vivo* models nanoparticles can be used to study, we studied 7C1 biodistribution and silencing in pulmonary epithelial cells, haematopoietic cells, T cells and B cells (Fig. 3a–c). We also measured gene silencing in hepatocytes and peritoneal immune cells, two cell types that have been preferentially transfected by lipid nanoparticles (Fig. 3d–f).

We quantified the uptake of Alexa647-labelled siRNA delivered by 7C1. One hour after a 1.0 mg kg^{-1} injection, lungs were digested into a single cell suspension and labelled with antibodies. Flow cytometry revealed that Alexa647 median fluorescent intensity was significantly higher in endothelial cells than in pulmonary epithelial cells, haematopoietic cells, T cells and B cells (Fig. 3a). Twenty-four hours after injection, endothelial cell uptake decreased. Although the significance of the decreased signal is unknown, it could result from fluorophore cleavage. We then used flow cytometry to simultaneously quantify ICAM-2 protein expression in pulmonary endothelial cells, haematopoietic cells, T cells and B cells. Three days following injection of 0.30, 0.20, 0.10 or 0.05 mg kg^{-1}, pulmonary endothelial cell ICAM-2 median fluorescent intensity decreased between 60% and 68% compared with cells from siCntrol treated mice (Fig. 3b). ICAM-2 median fluorescent intensity did not decrease in pulmonary haematopoietic cells, T cells or B cells. The relative delivery to lung endothelium and epithelium was then quantified with siRNA targeting Integrinß1 (Fig. 3c). Two days after injection, lung were digested before epithelial and endothelial cells were sorted into separate tubes with fluorescence activated cell sorting.

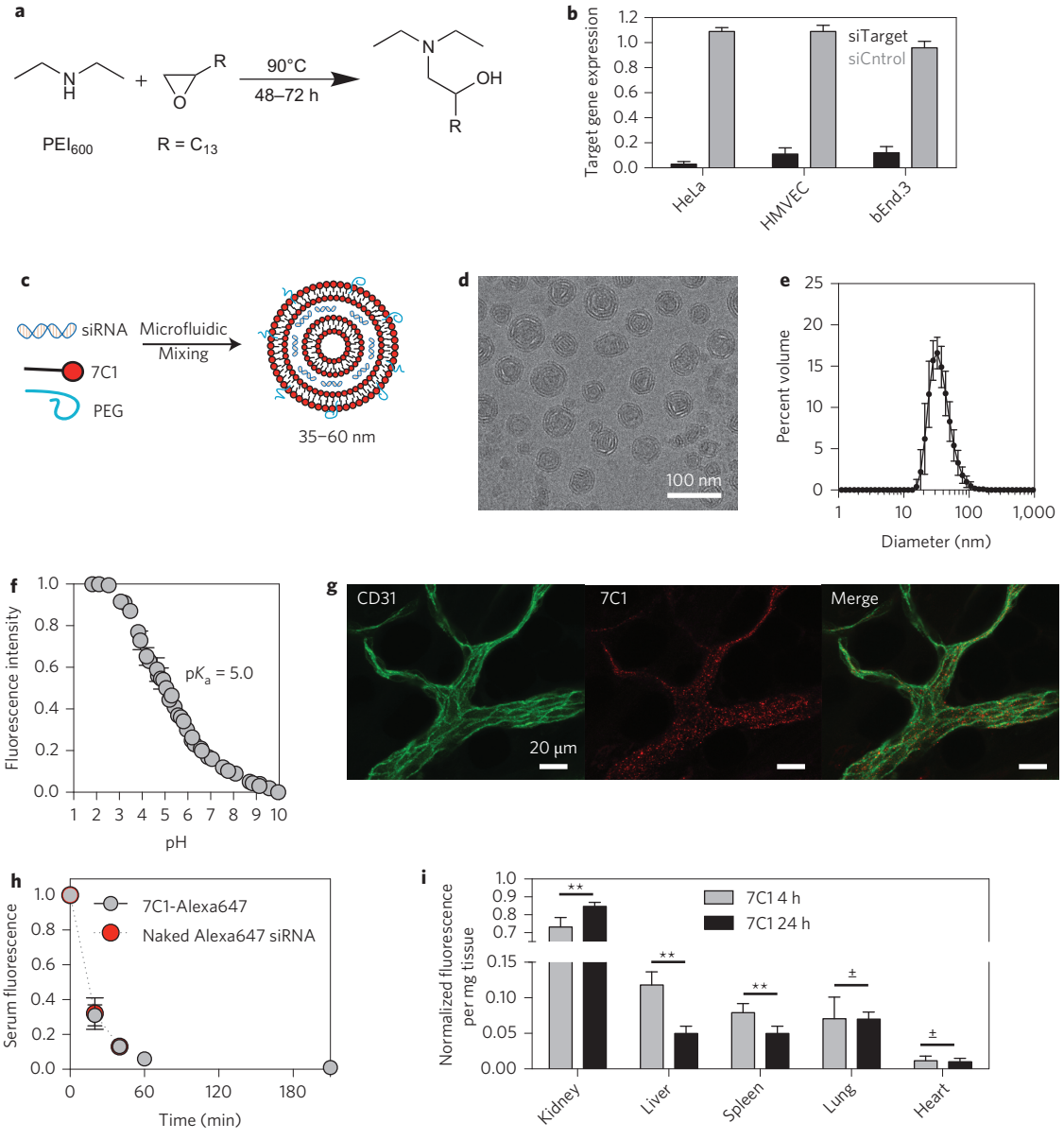

Figure 1 | 7C1 synthesis, characterization and *in vivo* biodistribution. a, 7C1 synthesis scheme. **b**, Target gene expression 24 h following 30 nM treatment with siRNA in human cervical carcinoma (HeLa), human primary endothelial (HMVEC) and murine endothelial (bEnd.3) cells. HeLa target gene expression was measured as Firefly luminescence in HeLa cells expressing Luciferase that were treated with siRNA targeting luciferase. bEnd.3 and HMVEC target gene expression was measured as Tie2 mRNA levels following treatment with siRNA targeting Tie2. **c**, 7C1 formulation scheme. 7C1 nanoparticles were mixed with $C_{14}PEG_{2000}$ and siRNA in a high-throughput microfluidic chamber as previously described[30]. **d**, 7C1 internal structure characterized by cryo-TEM. Dark bands indicate lipid layers and light bands indicate regions with siRNA. **e**, Average 7C1 hydrodynamic diameter, measured by dynamic light scattering, and weighted by volume ($N = 20$ formulations). **f**, 6,P-toluidinylnapthalene-2-sulfonate (TNS) fluorescence of formulated 7C1 nanoparticles as a function of pH (used to measure 7C1 pK_a). **g**, Representative confocal image of Alexa647-tagged siRNA complexed to 7C1 1 h after intravenous injection. CD31 is a ubiquitous marker for endothelium. **h**, Serum Cy5.5 concentration following injection with 7C1-Cy5.5 siRNA or naked Cy5.5 siRNA. **i**, Cy5.5 fluorescence per mg tissue after injection with 7C1-Cy5.5 siRNA. Tissues were removed after injection and weighed individually. Cy5.5 intensity was normalized to each individual tissue. Time points were selected to measure systemic siRNA accumulation after Cy5.5 was cleared from serum. $N = 4$–5 mice per group. In all cases, data are shown as mean ± s.d. $^{**}P < 0.005$, $^{\pm}P > 0.75$.

The purity of the sorted cells was confirmed by measuring cell-specific markers using RT–PCR (PCR with reverse transcription, Supplementary Fig. 2j). Compared with siCntrol-treated cells, endothelial cell Integrinß1 mRNA decreased by between 70% and 82%, while epithelial cell mRNA did not change substantially (Fig. 3c). These data indicate that, at these doses, 7C1 preferentially delivers siRNA to pulmonary endothelial cells.

We then analysed whether 7C1 delivered siRNA to hepatocytes, which are preferentially targeted by many lipid nanoparticle formulations (Fig. 3d). We measured the expression of a hepatocyte-specific gene Factor 7 (F7) after injection with the highly potent siF7[5]. F7 serum concentration remained constant after siF7 was injected at a dose of 1.5 mg kg^{-1} and was only reduced by 35% after an injection of 2.0 mg kg^{-1}, but the positive control lipid nanoparticle Hepat01 decreased F7 expression by 95% after a 0.30 mg kg^{-1} dose (Fig. 3d). To confirm that 7C1 reduced endothelial gene silencing without silencing hepatocyte gene expression, 7C1 was simultaneously complexed with siF7 and siTie2 (Fig. 3e).

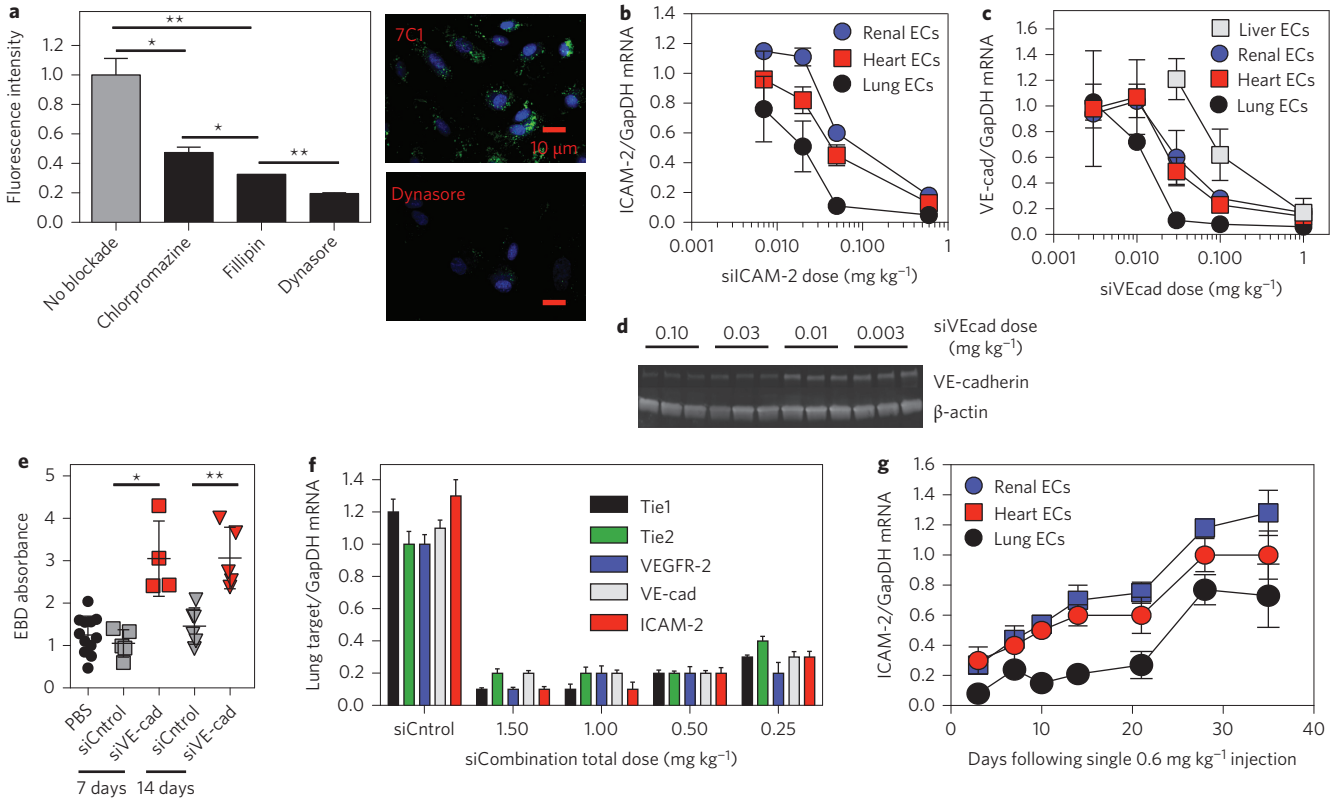

Figure 2 | 7C1 delivers siRNA to endothelial cells. a, Alexa647 fluorescence uptake in HMVEC cells following 7C1-Alexa647 treatment in the presence of small molecules inhibiting clathrin (Chlorpromazine), caveolin (Fillipin) and both endocytotic pathways (Dynasore). Representative images of cells treated with 7C1 or Dynasore are shown. **b**, ICAM-2/GapDH mRNA ratios (normalized to PBS-treated mice) following intravenous injection of 7C1-siICAM-2. **c**, VE-cadherin/GapDH mRNA ratios (normalized to PBS-treated mice) following intravenous injection of 7C1-siVEcad. **d**, VE-cadherin and β-actin protein expression following treatment with 7C1-siVEcad. **e**, Evans Blue Dye (EBD) pulmonary absorbance 7 and 14 days following a 0.6 mg kg^{-1} injection of 7C1-siVEcad. **f**, Target/GapDH mRNA ratios (normalized to PBS-treated mice) following injection of 7C1 formulated with siCntrol or five siRNAs targeting ICAM-2, Tie2, VE-cadherin, VEGFR2 or Tie1, respectively (siCombination). **g**, ICAM-2/GapDH mRNA levels as a function of time following a 0.6 mg kg^{-1} injection of siICAM-2. Data shown as mean ± s.d. $N = 4$–5 mice per group, $^{*}P < 0.05$, $^{**}P < 0.005$.

Because efficacy can vary with the molar ratio of PEG and cholesterol, we performed this two-gene experiment with particles formulated with different 7C1:cholesterol:$C_{14}PEG_{2000}$ molar ratios. Two formulations reduced lung Tie2 mRNA by nearly 90% after a single 0.15 mg kg^{-1} dose, but did not reduce *F7* expression (Fig. 3e).

Intravenously injected particles may also transfect peritoneal immune cells, especially CD11b^{+} monocytes and macrophages[22]. CD45 median fluorescent intensity was quantified in immune cells isolated from the peritoneal cavity following intravenous injection of 2.0 mg kg^{-1} 7C1 formulated with an siRNA targeting CD45 (siCD45)[22] (Fig. 3f). CD45 protein expression remained constant in macrophages, B cells, T cells and dendritic cells following treatment with 7C1 (Fig. 3f). By contrast, CD45 expression decreased in macrophages cells following treatment with the positive control lipid nanoparticle C12-200. Taken together, these data indicate that 7C1 does not deliver siRNA to hepatocytes or peritoneal immune cells in healthy BL/6 mice at any dose tested.

Endothelial RNAi affects multiple animal models

Whether RNA delivery could change endothelial function was then investigated in mouse models of emphysema, primary tumour growth and lung metastasis. Emphysema is characterized by decreased pulmonary surface area, which reduces gas transport, causing dyspnea and cough[23,24]. Along with macrophage-mediated protease imbalance, decreased VEGF and VEGFR-2 expression has been documented in the lungs of patients with chronic obstructive pulmonary disease. Moreover, genetic Cre-lox mediated deletion of VEGF causes emphysema in mice[24]. VEGF receptor blockade with SU5416 promotes emphysema in rodents, leading to decreased alveolar surface to volume ratios, increased lung volume and increased distance between alveolar walls (termed the mean linear intercept)[23]. Because SU5416 simultaneously inhibits VEGFR-1 and VEGFR-2, we characterized the pulmonary phenotype following VEGFR-2 specific silencing. VEGFR-2 silencing induced emphysema-like changes, indicated by decreased alveolar surface to volume ratios and increases in lung volume and mean linear intercept compared with siCntrol-treated mice (Fig. 3g–i,k). These changes were not due to infiltration of myeloid cells (Fig. 3j). These results suggest VEGFR-2 specific silencing is sufficient to induce emphysema-like phenotypes in mice and that systemic endothelial cell RNAi can be used to investigate the role of endothelial gene function *in vivo*.

The therapeutic effect of endothelial RNAi on primary tumour growth was then investigated in a Lewis lung carcinoma model. Previous work has demonstrated that antibodies targeting VEGFR-1 and Dll4 can reduce primary tumour growth through disrupted or non-productive angiogenesis, respectively[25,26]. In particular, targeting VEGFR-1, which is expressed on endothelial cells and pro-angiogenic myeloid cells, reduced tumour progression, metastasis and formation of a pre-metastatic niche[27,28]. However, monoclonal antibodies may function differently from RNAi-based methods, which inhibit both extracellular and intracellular signalling[29]. To investigate whether therapeutic deletion of VEGFR-1 and Dll4, both of which have intracellular signalling components,

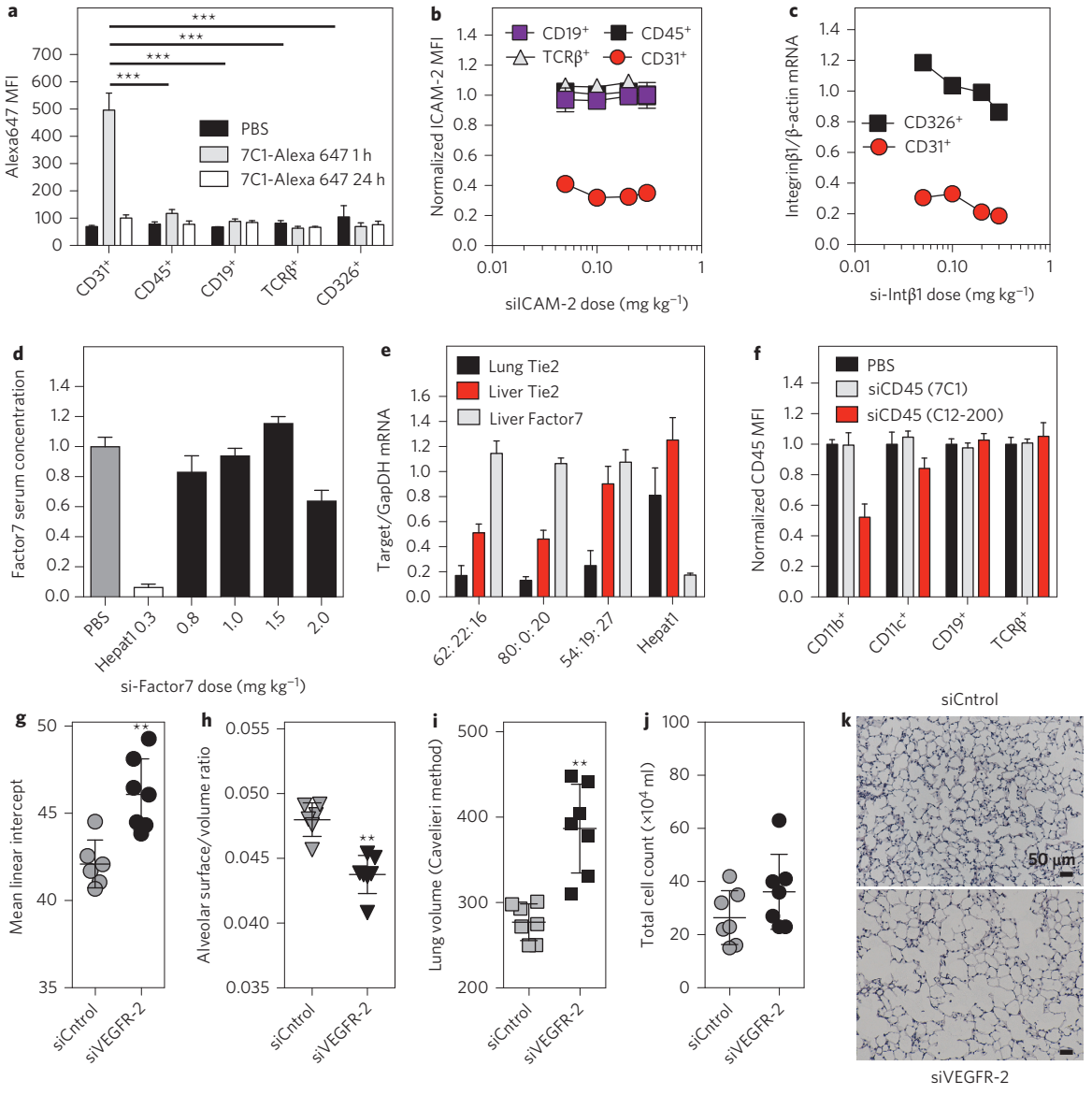

Figure 3 | 7C1 preferentially delivers siRNA to pulmonary endothelial cells *in vivo*. a, Alexa647 median fluorescent intensity in pulmonary endothelial ($CD31^+$), haematopoietic ($CD45^+$), epithelial ($CD326^+$), B ($CD19^+$) or T ($TCR\beta^+$) cells isolated from mice after treatment with 7C1 formulated with Alexa647-tagged siRNA. Statistical significance calculated between endothelial cells and other pulmonary cell types 1 h after injection. **b**, ICAM-2 median fluorescent intensity in pulmonary cells (normalized to siCntrol-treated mice) isolated from mice three days following treatment with 7C1-siICAM-2. **c**, Integrinβ1/β-actin mRNA ratios (normalized to siCntrol-treated mice) in pulmonary endothelial and epithelial cells isolated from mice two days after treatment with siIntegrinβ1. **d**, Factor 7 serum concentration (normalized to PBS-treated animals) two days following treatment with liver-targeting molecule Hepat01-siFactor7 or 7C1-siFactor7. **e**, Tie2 and Factor7/GapDH mRNA expression following a 0.15 mg kg^{-1} injection of 7C1 concurrently formulated with siTie2 and siFactor7. Particles were formulated with different 7C1:cholesterol:$C_{14}PEG_{2000}$ molar ratios. 7C1 decreased Tie2 mRNA expression in pulmonary, renal and hepatic endothelium without reducing F7 mRNA expression. **f**, CD45 median fluorescent intensity following treatment with 7C1-siCD45 or positive control C12-200-siCD45. **g–k**, Mean linear intercept (MLI) between alveoli, pulmonary surface/volume ratio, total volume and pulmonary histology following two 0.5 mg kg^{-1} injections of siCntrol or siVEGFR2. Increased MLI, alveolar volume, decreased surface/volume ratios and constant infiltrating myeloid cells are consistent with an induced emphysema-like phenotype ($N = 6$–7 animals per group; data shown as average ± s.d.). $^{**}P < 0.002$, $^{***}P < 0.001$.

would have similar effects as therapeutic antibodies, 7C1 was complexed with siCntrol, siVEGFR-1 or siDll4. Compared with siCntrol, siVEGFR-1 and siDll4 formulations had a significant therapeutic effect, reducing primary tumour growth by 40% and 70%, respectively, and increasing tumour necrosis (Fig. 4a–c). While some tumours treated with siVEGFR-1 exhibited high levels of cell death, others showed low levels[30]. These data suggest that targeted deletion of both the intracellular and extracellular portion of VEGFR-1 or Dll4 may reduce primary tumour growth.

The roles of VEGFR-1 and Dll4 in primary tumour growth have been studied extensively, but the role of these genes, particularly Dll4, in metastasis is less clearly understood[31,32]. Consequently, the effect of VEGFR-1 and Dll4 deletion on lung tumour metastases was studied in a metastatic Lewis lung carcinoma model (Fig. 4d,e, Supplementary Fig. 3). siVEGFR-1 reduced surface metastases by 52%, while siDll4 reduced surface metastases by 63% compared with siCntrol-treated mice (Fig. 4d,e). Lung weight, which correlates to the growth of lung metastases, decreased

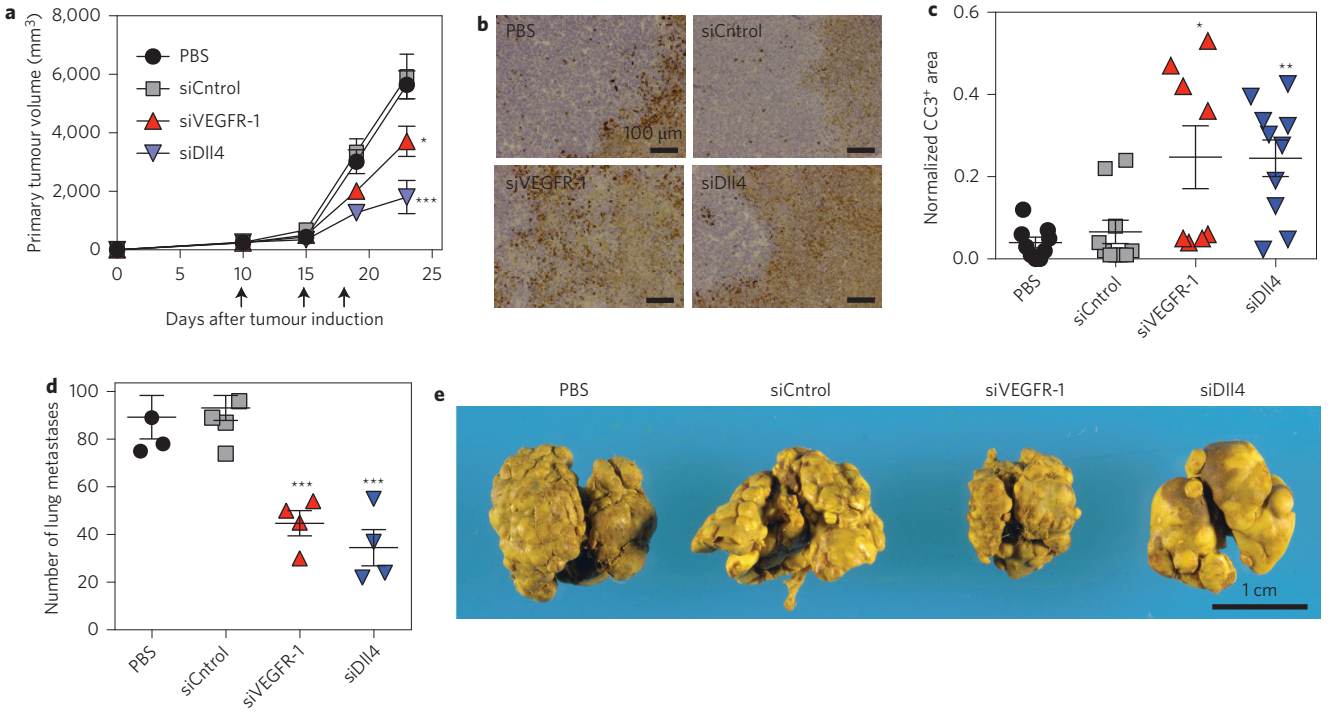

Figure 4 | 7C1-mediated mRNA silencing modifies endothelial function *in vivo*. **a**, Primary Lewis lung carcinoma (LLC) growth following three 1.0 mg kg^{-1} treatments with PBS, siCntrol, siVEGFR-1 or siDll4 ($N = 7$–10 animals per group; data shown as average ± s.e.m.). **b**,**c**, Representative images (**b**) and quantification of cleaved caspase 3 (CC3) staining (**c**), a marker for apoptosis, following treatment with PBS, siCntrol, siVEGFR-1, siDll4. Normalized CC3$^+$ area defined as the total CC3$^+$ surface area divided by the tumour surface area. **d**, Number of pulmonary surface metastases following four 1.0 mg kg^{-1} injections with PBS, siCntrol, siVEGFR-1 or siDll4 ($N = 4$–6 per group; data shown as average ± s.e.m.). To measure effects independent of primary tumour growth, animals were not treated until after primary tumour resection. **e**, Murine lungs with metastatic lesion removed after treatment with PBS, siLuc, siVEGFR-1 or siDll4. $^*P < 0.05$, $^{**}P < 0.002$, $^{***}P < 0.001$.

by 50% after siVEGFR-1 therapy and 60% after siDll4 therapy (Supplementary Fig. 3).

7C1 *in vivo* tolerability

7C1 nanoformulations were well tolerated in animal models of toxicity following acute and chronic high-dose treatment (Supplementary Fig. 4). We measured the serum concentrations of markers associated with toxicity after four 0.6 mg kg^{-1} intravenous injections in highly immunoactive CD1$^+$ mice, a mouse model used for preclinical toxicology studies. Mice were injected with a 0.6 mg kg^{-1} dose of siCntrol or siICAM-2 once a week for four weeks. Forty-eight hours after the last injection, the serum concentrations of markers for hepatic, cardiovascular and renal injury were quantified. Importantly, we observed no evidence of kidney damage (Supplementary Fig. 4a).

7C1 tolerability was also investigated in BL/6 mice at doses much higher than those required for functional gene silencing (2 mg kg^{-1}) in acute and chronic models. Over 28 days, mice were injected eight times with PBS solution or 2 mg kg^{-1} 7C1. Murine weight gain equalled that of mice injected with PBS (Supplementary Fig. 4b). Four hours after the final injection, mice were killed and lungs were removed before mRNA expression of cytokines (IL-6, TNF-α), markers of endothelial dysfunction (ICAM-2, E-selectin) and immune cell infiltration (CD45) were quantified (Supplementary Fig. 4c). Serum concentrations of 30 cytokines were also quantified. mRNA expression and cytokine concentration did not increase significantly when compared to PBS-treated mice (Supplementary Fig. 4d).

We then measured serum cytokine concentration 2, 4, 6 and 24 h following a 2.0 mg kg^{-1} injection. Although the serum concentrations of five factors did increase between 2 and 6 h, only one factor (CXCL2) equalled the concentration in mice treated with a low-dose lipopolysaccharide (LPS) control and all five returned to baseline 24 h after injection (Supplementary Fig. 4e). These data suggest that, while 7C1 probably interacts with cells to produce a transient response at doses much higher than those required for gene silencing, the formulation appears to be well tolerated in multiple mouse models *in vivo*.

Conclusions

We have identified a nanoparticle (7C1) that efficiently delivers siRNA to endothelial cells. Unlike previously reported lipid and lipidoid-based nanoparticles, 7C1 transfected endothelial cells *in vivo* at low doses, without significantly reducing gene expression in hepatocytes, peritoneal immune cells, pulmonary epithelial cells or pulmonary immune cells. The exact molecular mechanism governing this effect remains to be determined, but it seems to involve the interaction of 7C1 with serum proteins, which can promote delivery to certain cell types[33]. As a result, 7C1 may be an interesting system to study how physiochemical interactions between nanomaterials and serum proteins direct nanoparticles to endothelial cells *in vivo*[34–37]. This nanoformulation enables the simultaneous silencing of multiple endothelial genes. Although some immune cells are known to express Tie1, Tie2 and ICAM-2, the lack of significant pulmonary immune cell gene silencing (mediated by 7C1) indicates that such multigene silencing occurs primarily in endothelial cells. We therefore anticipate that 7C1 can be useful in the study of gene combinations in complex biological pathways *in vivo*, a strategy called *in vivo* genomics.

Moreover, we have found that 7C1 reduces primary tumour growth and lung metastases in a model of lung cancer. As a result, although this study examined targets whose extracellular

activity can also be inhibited by antibodies, future therapies may be designed to target combinations of proteins currently considered 'undruggable'. Similarly, future RNA therapies may enhance the effects of non-RNA drugs (for example, modifying the expression of the gene involved in the exocytosis of a small molecule might enhance its delivery).

Finally, we have shown that 7C1 durably reduces target gene expression in multiple animal models. This extended therapeutic effect may increase the utility of *in vivo* endothelial RNAi. Because 7C1 is well tolerated at doses far higher than those required for gene silencing, we believe this technology will be used to manipulate gene expression *in vivo*. In summary, 7C1 nanoformulations should provide biologists and engineers with a new tool to efficiently deliver siRNA to endothelium.

Received 1 August 2013; accepted 25 March 2014;
published online 11 May 2014; corrected online 20 June 2014

References

1. Pober, J. S. & Sessa, W. C. Evolving functions of endothelial cells in inflammation. *Nature Rev. Immunol.* **7,** 803–815 (2007).
2. Hagberg, C. E. *et al.* Targeting VEGF-B as a novel treatment for insulin resistance and type 2 diabetes. *Nature* **490,** 426–430 (2012).
3. Kumar, V., Abbas, A., Fausto, N. & Aster, J. *Robbins and Cotran Pathologic Basis of Disease* 8th edn (Elsevier, 2009).
4. Kanasty, R., Dorkin, J. R., Vegas, A. & Anderson, D. Delivery materials for siRNA therapeutics. *Nature Mater.* **12,** 967–977 (2013).
5. Love, K. T. *et al.* Lipid-like materials for low-dose, *in vivo* gene silencing. *Proc. Natl Acad. Sci. USA* **107,** 1864–1869 (2010).
6. Semple, S. *et al.* Rational design of cationic lipids for siRNA delivery. *Nature Biotechnol.* **28,** 172–176 (2010).
7. Whitehead, K. A., Langer, R. & Anderson, D. G. Knocking down barriers: advances in siRNA delivery. *Nature Rev. Drug Discov.* **8,** 129–138 (2009).
8. Aleku, M. *et al.* Atu027, a liposomal small interfering RNA formulation targeting protein kinase N3, inhibits cancer progression. *Cancer Res.* **68,** 9788–9798 (2008).
9. Aleku, M. *et al.* Intracellular localization of lipoplexed siRNA in vascular endothelial cells of different mouse tissues. *Microvasc. Res.* **76,** 31–41 (2008).
10. Santel, A. *et al.* RNA interference in the mouse vascular endothelium by systemic administration of siRNA-lipoplexes for cancer therapy. *Gene Ther.* **13,** 1360–1370 (2006).
11. Santel, A. *et al.* A novel siRNA-lipoplex technology for RNA interference in the mouse vascular endothelium. *Gene Ther.* **13,** 1222–1234 (2006).
12. Polach, K. J. *et al.* Delivery of siRNA to the mouse lung via a functionalized lipopolyamine. *Mol. Ther.* **20,** 91–100 (2012).
13. Kaufmann, J., Ahrens, K. & Santel, A. RNA interference for therapy in the vascular endothelium. *Microvasc. Res.* **80,** 286–293 (2010).
14. Davis, M. E. *et al.* Evidence of RNAi in humans from systemically administered siRNA via targeted nanoparticles. *Nature* **484,** 1067–1070 (2010).
15. Rozema, D. B. *et al.* Dynamic polyconjugates for targeted *in vivo* delivery of siRNA to hepatocytes. *Proc. Natl Acad. Sci. USA* **104,** 12982–12987 (2007).
16. Godbey, W. T., Wu, K. K. & Mikos, A. G. Poly(ethylenimine) and its role in gene delivery. *J. Control. Rel.* **60,** 149–160 (1999).
17. Breunig, M., Lungwitz, U., Liebl, R. & Goepferich, A. Breaking up the correlation between efficacy and toxicity for nonviral gene delivery. *Proc. Natl Acad. Sci. USA* **104,** 14454–14459 (2007).
18. Richards Grayson, A. C., Doody, A. M. & Putnam, D. Biophysical and structural characterization of polyethylenimine-mediated siRNA delivery *in vitro*. *Pharm. Res.* **8,** 1868–1876 (2006).
19. Crawford, R. *et al.* Analysis of lipid nanoparticles by cryo-EM for characterizing siRNA delivery vehicles. *Int. J. Pharm.* **403,** 237–244 (2011).
20. Jayaraman, M. *et al.* Maximizing the potency of siRNA lipid nanoparticles for hepatic gene silencing *in vivo*. *Angew. Chem. Int. Ed.* **51,** 8529–8533 (2012).
21. Huang, H., Bhat, A., Woodnutt, G. & Lappe, R. Targeting the ANGPT-TIE2 pathway in malignancy. *Nature Rev. Cancer* **10,** 575–585 (2010).
22. Novobrantseva, T. I. *et al.* Systemic RNAi-mediated gene silencing in nonhuman primate and rodent myeloid cells. *Mol. Ther. Nucleic Acids* **1,** e4 (2012).
23. Kasahara, Y. *et al.* Inhibition of VEGF receptors causes lung cell apoptosis and emphysema. *J. Clin. Invest.* **106,** 1311–1319 (2000).
24. Tuder, R. M. & Yun, J. H. Vascular endothelial growth factor of the lung: friend or foe. *Curr. Opin. Pharmacol.* **8,** 255–260 (2008).
25. Thurston, G., Noguera-Troise, I. & Yancopoulos, G. D. The Delta paradox: DLL4 blockade leads to more tumour vessels but less tumour growth. *Nature Rev. Cancer* **7,** 327–331 (2007).
26. Fischer, C., Mazzone, M., Jonckx, B. & Carmeliet, P. FLT1 and its ligands VEGFB and PlGF: drug targets for anti-angiogenic therapy? *Nature Rev. Cancer* **8,** 942–956 (2008).
27. Lyden, D. *et al.* Impaired recruitment of bone-marrow-derived endothelial and hematopoietic precursor cells blocks tumor angiogenesis and growth. *Nature Med.* **7,** 1194–1201 (2001).
28. Kaplan, R. N. *et al.* VEGFR1-positive haematopoietic bone marrow progenitors initiate the pre-metastatic niche. *Nature* **438,** 820–827 (2005).
29. Tammela, T. *et al.* VEGFR-3 controls tip to stalk conversion at vessel fusion sites by reinforcing Notch signalling. *Nature Cell Biol.* **13,** 1202–1213 (2011).
30. Stevens, J. B. *et al.* Heterogeneity of cell death. *Cytogenet. Genome Res.* **139,** 164–173 (2013).
31. Kuramoto, T. *et al.* Dll4-Fc, an inhibitor of Dll4-notch signaling, suppresses liver metastasis of small cell lung cancer cells through the downregulation of the NF-kappaB activity. *Mol. Cancer Ther.* **11,** 2578–2587 (2012).
32. Garcia, A. & Kandel, J. J. Notch: a key regulator of tumor angiogenesis and metastasis. *Histol. Histopathol.* **27,** 151–156 (2012).
33. Akinc, A. *et al.* Targeted delivery of RNAi therapeutics with endogenous and exogenous ligand-based mechanisms. *Mol. Ther.* **18,** 1357–1364 (2010).
34. Monopoli, M. P., Aberg, C., Salvati, A. & Dawson, K. A. Biomolecular coronas provide the biological identity of nanosized materials. *Nature Nanotech.* **7,** 779–786 (2012).
35. Chen, D. *et al.* Rapid discovery of potent siRNA-containing lipid nanoparticles enabled by controlled microfluidic formulation. *J. Am. Chem. Soc.* **134,** 6948–6951 (2012).
36. Whitehead, K., Dahlman, J. E., Langer, R. S. & Anderson, D. G. Silencing or stimulation? siRNA delivery and the immune system. *Ann. Rev. Chem. Biomol. Eng.* **2,** 77–96 (2011).
37. Panigrahy, D. *et al.* Epoxyeicosanoids stimulate multiorgan metastasis and tumor dormancy escape in mice. *J. Clin. Invest.* **122,** 178–191 (2012).

Acknowledgements

The authors thank J. Cattie, T. O'Shea and T. Tammela. J.E.D. was supported by National Defense Science and Engineering (NDSEG), the National Science Foundation (NSF) and MIT Presidential Fellowships. D.P. was supported by R01 CA148663. M.W.K. was supported by the Stop and Shop Pediatric Brain Tumour Fund, as well as the Pediatric Brain Tumour Fund. H.S. was supported by the Deutsche Forschungsgemeinschaft (SA1668/2-1). Research was also supported by Alnylam and the Center for RNA Therapeutics and Biology.

Author contributions

J.E.D., C.B., V.K., R.L. and D.G.A. conceived the experiments. J.E.D., C.B., O.F.K., A.T., S.J., T.E.S., Y.X., H.B.S., G.S., L.S., A.B., R.L.B., H.Y., T.R., Y.D., S.J., D.S., A.D., K.S.S., M.J.W., T.N., V.M.R., A.K.R.L.J., C.G.L., B.K., D.K.M., M.P., L.A., P.D., L.S., K.C., M.W.K., K.F., M.N., D.D., R.M.T., U.H.V.A., A.A., A.S. and D.P. performed experiments. J.E.D., C.B., V.K., R.L. and D.G.A. co-wrote the paper. All authors discussed the results and commented on the manuscript.

Additional information

Supplementary information is available in the online version of the paper. Reprints and permissions information is available online at www.nature.com/reprints. Correspondence and requests for materials should be addressed to D.G.A.

Competing financial interests

R.L. is a shareholder and member of the Scientific Advisory Board of Alnylam. R.L and D.G.A have sponsored research grants from Alnylam. Alnylam also has a licence to certain intellectual property that was invented at the Massachusetts Institute of Technology by D.G.A. and R.L.

James E. Dahlman[1,2,3†], Carmen Barnes[4†], Omar F. Khan[2,5], Aude Thiriot[6], Siddharth Jhunjunwala[2], Taylor E. Shaw[2], Yiping Xing[2], Hendrik B. Sager[7], Gaurav Sahay[2], Lauren Speciner[4], Andrew Bader[2], Roman L. Bogorad[2], Hao Yin[2], Tim Racie[4], Yizhou Dong[2], Shan Jiang[2], Danielle Seedorf[2], Apeksha Dave[2], Kamaljeet Singh Sandhu[2], Matthew J. Webber[2], Tatiana Novobrantseva[4], Vera M. Ruda[2], Abigail K. R. Lytton-Jean[2], Christopher G. Levins[2], Brian Kalish[8], Dayna K. Mudge[8], Mario Perez[9], Ludmila Abezgauz[10], Partha Dutta[7], Lynelle Smith[9], Klaus Charisse[4], Mark W. Kieran[6], Kevin Fitzgerald[4], Matthias Nahrendorf[7], Dganit Danino[10], Rubin M. Tuder[9], Ulrich H. von Andrian[6], Akin Akinc[4], Dipak Panigrahy[6], Avi Schroeder[11], Victor Koteliansky[12], Robert Langer[1,2,3,5] and Daniel G. Anderson[1,2,3,5]*

[1]Harvard-MIT Division of Health Sciences and Technology, Massachusetts Institute of Technology, Cambridge, Massachusetts 02139, USA. [2]David H. Koch Institute for Integrative Cancer Research, Massachusetts Institute of Technology, Cambridge, Massachusetts 02139, USA. [3]Institute for Medical Engineering and Science, Massachusetts Institute of Technology, Cambridge, Massachusetts 02139, USA. [4]Alnylam Pharmaceuticals, Cambridge, Massachusetts 02139, USA. [5]Department of Chemical Engineering, Massachusetts Institute of Technology, Cambridge, Massachusetts 02139, USA. [6]Department of Microbiology and Immunology, Harvard Medical School, Boston 02115, USA. [7]Center for Systems Biology, Massachusetts General Hospital and Harvard Medical School, Boston 02114, USA. [8]Vascular Biology Program, Children's Hospital Boston, and Division of Pediatric Oncology, Dana Farber Cancer Institute, Harvard Medical School, Boston 02115, USA. [9]Program in Translational Lung Research, Division of Pulmonary Sciences and Critical Care Program, Department of Medicine, University of Colorado School of Medicine, USA. [10]Department of Biotechnology and Food Engineering and The Russell Berrie Nanotechnology Institute, Technion Israel Institute of Technology, Haifa 3200, Israel. [11]Department of Chemical Engineering, Technion Israel Institute of Technology, Haifa 32000, Israel. [12]Skolkovo Institute of Science and Technology, Skolkovo 143025, Russian Federation. [†]These authors contributed equally to this work.
*e-mail: dgander@mit.edu

CORRIGENDUM

In vivo endothelial siRNA delivery using polymeric nanoparticles with low molecular weight

James E. Dahlman, Carmen Barnes, Omar F. Khan, Aude Thiriot, Siddharth Jhunjunwala, Taylor E. Shaw, Yiping Xing, Hendrik B. Sager, Gaurav Sahay, Lauren Speciner, Andrew Bader, Roman L. Bogorad, Hao Yin, Tim Racie, Yizhou Dong, Shan Jiang, Danielle Seedorf, Apeksha Dave, Kamaljeet Singh Sandhu, Matthew J. Webber, Tatiana Novobrantseva, Vera M. Ruda, Abigail K. R. Lytton-Jean, Christopher G. Levins, Brian Kalish, Dayna K. Mudge, Mario Perez, Ludmila Abezgauz, Partha Dutta, Lynelle Smith, Klaus Charisse, Mark W. Kieran, Kevin Fitzgerald, Matthias Nahrendorf, Dganit Danino, Rubin M. Tuder, Ulrich H. von Andrian, Akin Akinc, Dipak Panigrahy, Avi Schroeder, Victor Koteliansky, Robert Langer and Daniel G. Anderson

Nature Nanotechnology http://dx.doi.org/10.1038/nnano.2014.84 (2014); published online 11 May 2014; corrected online 20 June 2014.

In the version of this Article originally published online, the following authors' names were written incorrectly: Victor Koteliansky, Omar F. Khan and Kamaljeet Singh Sandhu. These have now been corrected in all versions of the Article.